Nanoscale Horizons

ROYAL SOCIETY OF CHEMISTRY

COMMUNICATION

View Article Online
View Journal | View Issue

Cite this: *Nanoscale Horiz.*, 2026, **11**, 170

Received 21st August 2025,
Accepted 10th October 2025

DOI: 10.1039/d5nh00597c

rsc.li/nanoscale-horizons

Low-energy synthesis of individualized pH-responsive cationic cellulose nanofibers and chitin nanocrystals by mechanochemistry and aging

Galen Yang, [ab] Yuka Tomita, [b] Austin J. Richard, [a] Shuji Fujisawa, [b] Edmond Lam, [a] Tsuguyuki Saito [b] and Audrey Moores *[abc]

Cellulose and chitin nanomaterials are promising sustainable materials that exhibit attractive mechanical, optical, thermal, and chemical properties. Cellulose nanofibers (CNFs) have found applications to the field of packaging, reinforced composite or biomedical applications. Introducing charged functional groups onto these nanomaterials is a proven strategy to improve their dispersibility and processability, as well as their properties, such as adsorption capacity. The use of high energy defibrillators has remained necessary to access CNFs despite the introduction of surface charges prior to increase the efficiency of nanomaterial extraction. To date, there is no known synthesis of cationic CNFs (CCNFs) that is both energy efficient in the defibrillation, and chemically efficient in material modification. Herein we report a strategy to access CCNFs directly from once-dried wood pulp through mechanochemical and aging-based nucleophilic substitution, followed by a short sonication. This treatment introduces pH-responsive cationic diethylethylamine (DEEA) groups with a degree of substitution (DS) as high as 0.80 (amine content of 3.29 mmol g^{-1}) without the use of excess reagents. The combination of short mechanochemical treatment (10 min), with aging (3 h) and sonication (5 min) allows rapid access to high quality, 2-nm-wide, 1-μm-long CCNFs with high crystallinity of 56.6% and high ζ-potential of 68.10 ± 1.43 mV from sheets of pulp. The method was also applied to powder microcrystalline cellulose and chitin, to afford cationic nanocrystals of cellulose and chitin.

New concepts

This work introduces a breakthrough in nanocellulose synthesis by leveraging mechanochemistry to directly graft tertiary amines onto once-dried pulp, enabling unprecedentedly low-energy defibrillation. Unlike conventional methods that rely on high-pressure homogenization or extensive chemical pretreatment, our approach achieves high degrees of substitution (up to 3.29 mmol g^{-1}) through a brief ball-milling and aging process, followed by minimal sonication. This strategy not only preserves crystallinity but also yields individualized, high-aspect-ratio cationic cellulose nanofibers (CCNFs) with record-high ζ-potentials, promoting colloidal stability and pH responsiveness. The innovation lies in the direct solid-state functionalization of native biomass, bypassing energy-intensive steps and unlocking scalable access to CCNFs and chitin nanocrystals. By demonstrating that mechanochemistry can drive efficient S_N2-type reactions in complex polysaccharide matrices, this work expands the toolbox of sustainable materials processing and opens new avenues for functional nanomaterials in water treatment, responsive hydrogels, and bio-based composites.

Audrey Moores

I am a Full Professor of Chemistry at McGill University and associate director of the Facility for Electron Microscopy Research. My research focuses on sustainable nanomaterials and biopolymer synthesis. I previously co-authored a Nanoscale Horizons review on chitin and chitosan nanomaterials that helped introduce these emerging bio-based systems to the wider nanoscience community. It is a pleasure to contribute again to the journal's 10th-anniversary issue and to celebrate a decade of inspiring research shaping the future of nanoscale science and sustainability.

Introduction

Cellulose nanofibers (CNFs) are a class of materials produced by the mechanical disentanglement of cellulose microfibrils

[a] *Centre in Green Chemistry and Catalysis, Department of Chemistry, McGill University, 801 Sherbrooke St. West, Montreal, QC, H3A 0B8, Canada. E-mail: Audrey.moores@mcgill.ca*
[b] *Department of Biomaterial Sciences, Graduate School of Agricultural and Life Sciences, The University of Tokyo, 1-1-1 Yayoi, Bunkyo-ku, Tokyo 113-8657, Japan*
[c] *Department of Materials Engineering, McGill University, 3610 University Street, Montreal, Quebec H3A 0C5, Canada*

that exist, bundled, in the cell walls of plants or the extracellular cellulose of bacteria.[1–3] It is a sustainable material obtained from a regenerative feedstock with an annual availability over 1.5 trillion tonnes.[4] CNFs are composed of crystalline polymeric chains of cellulose, made of repeated β(1 → 4) linked D-glucose units, either in its pristine form or chemically modified,[3,5] and feature attractive properties,[6] for example flame retardancy for phosphorylated CNFs,[7] high hydrophobicity for acetylated CNFs,[8] and widely reported ability in facilitating organic reactions.[9] They are lightweight yet physically strong and stiff with a theoretical strength of 4.7 GPa, higher than most synthetic materials including polymers, metal alloys, and ceramics.[10–12] CNFs can also be processed into transparent structural materials with great thermal dimensional stability.[13–15] Furthermore, individual CNFs have great colloidal stability and are able to form a homogenous suspension when dispersed in water.[1] CNFs are generally hydrophilic, thanks to native and process-acquired functional groups (hydroxyl, carboxylic, phosphoryl, sulfonyl *etc.*), yet the (2 0 0) crystalline planes of CNFs enable hydrophobic–hydrophobic interactions, providing CNFs with remarkable emulsification capacity in Pickering emulsions.[16,17] In addition, CNFs also exhibit great potential in water treatment as either an adsorbent or flocculant.[18,19] Therefore, CNFs are regarded as a key material for sustainable technologies.[20–22]

CNFs are typically produced by high-pressure (HP) homogenization. While it is a very effective method to yield long and well defined CNFs, it often requires an energy intensive process, with over 1000 bar of pressure necessary to break the interfacial hydrogen bonds between cellulose fibrils,[23,24] and overcome dispersion interactions.[25] CNFs synthesis can be effectively facilitated through chemical modification prior to defibrillation. TEMPO (2,2,6,6-tetramethylpiperidine-1-oxylradical) oxidation is the benchmark method for preparing fibrillated, anionic CNFs from native cellulose.[1] The oxidation of cellulose surface C6 hydroxyl group to carboxylate groups occur during TEMPO-oxidation, with β-elimination of the aldehyde intermediate under alkaline condition taking place simultaneously and causing shortening of resulting cellulose fibrils.[26] Electric double layer repulsion governed by the anionic surface carboxylates generated during TEMPO-oxidation promotes fiber separation, allowing defibrillation to take place by ultrasonication with significantly reduced mechanical force.[27] TEMPO-oxidation provided a simple yet reliable process for anionic TEMPO-oxidized CNFs, making up 54.1% of the global CNFs production at a value of US$2.4 billion in 2023.[28] Similar approaches for the modification of cellulose with anionic functional groups include phosphorylation,[29] phosphite esterification,[30] carboxymethyl etherification,[31] xanthate esterification,[32] alkenylsuccinate esterification,[33] and sulfate esterification.[34]

In contrast to anionic CNFs, the cationic CNFs (CCNFs) synthesis has yet to see its eureka moment (see discussion S1 in SI). The existing CCNFs syntheses can be categorized as either the pre-functionalization approach, where pulp is grafted with cationic amine group, before mechanical defibrillation;[35–43] or the post-functionalization approach, where the amine-modification is made on already formed CNFs.[44–46] To the best of our knowledge, all studies related to the pre-functionalization approach reference to the work by Pei *et al.* from 2013.[35] In the method described, beaten, never-dried softwood sulphite pulp in a 5 wt% NaOH solution mixed with glycidyltrimethylammonium chloride (GTMAC) at 65 °C for 8 h led to S_N2-attack on surface hydroxyl groups. After reaction and purification, the cationic pulp was dispersed in water at 0.5% (w/v) and underwent HP homogenization of 1600 bar. The process resulted in CCNFs with fiber width in the range of 1.6–2.1 nm, fiber length in the range of 1.3–2.0 μm, and a crystallinity index (CrI) in the range of 61–65%. Although the authors provided quantified trimethylammonium chloride contents as high as 2.3 mmol g^{-1}, the reaction efficiency could not be calculated as the amount of GTMAC used was not disclosed. In spite of its low reaction efficiency exposed in the follow-up studies where the synthesis was employed, the resulting CCNFs have been shown to be effective in pollutant removal studies,[35–42] including for perfluoroalkyl and polyfluoroalkyl substances (PFAS) adsorption, a notoriously challenging substrate to trap.[36] Therefore, a pre-functionalized CCNFs synthesis that exhibits both high reaction efficiency in chemical modification and does not require energy intensive HP homogenization is urgently needed.

Beside CNFs materials, polysaccharide nanocrystals are another important class of nanomaterials directly accessible from biomass. Both cellulose and chitin nanocrystals (CNC and ChNC) can be accessed by the chemical selective depolymerization of cellulose pulp or chitin, respectively, and are characterized by smaller aspect ratio compared to nanofibers, with typical width of 5–10 nm and length of 100–300 nm. While the defibrillation of unmodified polysaccharides is easier to achieve than in the case of CNFs due to the smaller adhesion surfaces between strands of crystals *vs.* longer fibers,[47,48] surface modification such as TEMPO-oxidation remains an effective strategy for the design, synthesis and stability of CNCs and ChNCs.[49] What is unique about ChNCs is that partial deacetylation can lead to the formation of cationic chitosan nanocrystals (ChsNCs), which possess surface amine functionalities.[50,51] In contrast, introducing analogous amine functionalities onto CNCs typically requires less efficient post-functionalization approach, such as heterogeneous S_N2 reactions in DMSO dispersions.[52] Yet other possibilities such as organosilanization with aminotrimethoxysilanes,[53] reductive amination of oxidative ring-opened dialdehyde cellulose,[54] or EDC/NHS coupling of oxidized cellulose with diamines have only been applied on bulk cellulose.[55]

Mechanochemical reactions are defined as a chemical reactions that are induced by the direct absorption of mechanical energy,[56–58] and rely on equipment such as conventional mortar and pestle,[59] ball mills,[60,61] extruders,[62,63] and resonant acoustic mixing (RAM).[64,65] On the other hand, aging, or accelerated aging, is a strategy used in conjunction to mechanochemistry in a scheme in which ball-milled materials is let to age at room temperature (RT) or moderate heating, under dry

atmosphere, high humidity or the presence of vapours of a reagent of choice.[66–71] These techniques have been applied to the production and functionalization of nanopolysaccharides. Our group has demonstrated their efficacy in obtaining ChsNCs,[51] as well as carboxylated CNCs, and ChNCs through mechanochemical grinding, followed by stationary or high-humidity shaker aging, and finalized with low-energy ultrasonication.[72] The mechanochemical functionalization of CNCs has also been shown in our work on phosphorylated CNCs, prepared by 30 min ball-milling with phosphorus pentoxide and urea.[73] More demanding grafting reactions require longer milling times, such as the 6 h treatment reported by Wei and coworkers for the esterification of CNFs with acylimidazoles to obtain lipophilic CNFs.[74] Aging, however, has shown promise in reducing milling requirements: Langerreiter and coworkers synthesized amine-modified CNCs with modest amine contents (0.3 mmol g^{-1}) *via* two milling steps (65 min total) followed by aging, using tosylation and nucleophilic substitution on acid-hydrolyzed CNCs.[75] While these strategies are successful in affording good functionalization, prolonged ball-milling of crystalline polysaccharides has the propensity to cause significant amorphization or damage to the crystals,[72,76,77] which can negatively affect the properties of polysaccharide nanomaterials made with this technique.[51] More recently, our group developed synthetic strategies using bulk polysaccharide substrates in which the milling step is minimized to favor aging as the main reaction step.[78,79] This was very effective for the functionalization of bulk chitosan with aldehydes[80] as well as with electrophiles.[81] In the latter case, aging after 30 min milling enabled the same high degree of substitution (DS) in the S_N2-type aminoalkylation reaction with only 30 min of milling instead of 3 h, effectively affording the synthesis of highly loaded positively charged chitosan. With further optimization, this process appeared as a great starting point for accessing from cellulose novel CCNFs with high charge, high quality and a reduced energy demand.

Herein, we present a method of synthesizing CCNFs with high amine content, through low energy mechanochemistry, aging and sonication steps. This method provides access to high aspect ratio CCNFs and cationic ChNCs with average particle width of 2 nm and length depending on the substrate ($\sim$1 μm with wood pulp, $\sim$400 nm with practical grade chitin). Record-high amine contents over 3 mmol g^{-1} provided the nanopolysaccharides with strong electric double layer repulsion and colloidal stability. We then examined the pH responsiveness of CCNFs and found high pH over 8.5 reduced the repulsion by deprotonating the surface amines and afforded rigid hydrogels.

Results and discussion

Solid-phase S_N2 type functionalization of cellulose and chitin

In earlier work,[81] we developed a mechanochemical and aging-based nucleophilic substitution reaction on chitosan with 2-chloro-*N*,*N*-dimethylethylamine (CDMEA) as the electrophile. Importantly, both C2-primary amines and C6-primary alcohol functionalities on chitosan were available for alkylation. We applied this reaction to both cellulose and chitin, noting that these polysaccharides would only have their C6-primary alcohol available for reaction (and possibly less than 5% of deacetylated amine present in native chitin). While both substrates share the same C6 hydroxyl nucleophile for this transformation, the C2 acetamide groups in chitin engage in strong interchain hydrogen bonding, leading to higher crystallinity and reduced susceptibility to chemical modification. By comparing these two distinct polysaccharides, we aimed to evaluate the versatility and general applicability of the S_N2-type aminoalkylation method on crystalline polysaccharide substrates. For reaction optimization, powdered microcrystalline cellulose (MCC) or practical grade (PG) chitin were used as reagents, loaded along with CDMEA·HCl and NaOH in polytetrafluoroethylene (PTFE) jars with a 7 mm ZrO_2 ball. Tetrabutylammonium hydroxide (TBAH) in solution was added to the powder, producing liquid-assisted grinding (LAG) conditions for this reaction. The reaction mixture was milled at 29.5 Hz for 30 min followed by 2 d of RT aging. Such condition was chosen because in our previous work, we found that ball-milling a tertiary ammonium hydrochloride salt with NaOH generates the volatile, reactive chloroalkyl tertiary amine electrophile *in situ*, to react with chitosan with TBAH as a catalyst.[81] The resulting reaction mixture after milling and aging was purified by dialysis in deionized (DI) water and freeze-dried for storage and characterization. The efficacy of the solid-state modification in term of DS was evaluated with ^{13}C magic angle spinning nuclear magnetic resonance (ssNMR) spectroscopy. Unlike amorphous chitosan, which afforded high DS (calculated based on the average number of grafted structures per monosaccharide rings) under these reaction conditions, crystalline MCC and PG chitin were recovered virtually unreacted, with low DS of 0.02 and 0.00, respectively.

To improve the DS values, we explored other similar tertiary amine-containing electrophiles including 3-chloro-*N*,*N*-dimethylpropylamine (CDMPA) and 2-chloro-*N*,*N*-diethylethylamine (CDEEA) for reaction with MCC. Although CDMPA did not afford any noticeable DS to MCC, when CDEEA was used as the electrophile, we found the S_N2-type reaction proceeded well, and DEEA were grafted onto the primary alcohol groups of MCC under tested conditions.[81] The resulting material was named DEEA-MCC. We proceeded to optimize the reaction conditions by varying milling time from 5, 10, and 30 min and aging time between 3 and 48 h, for the synthesis of aminoalkylated crystalline polysaccharides (Scheme 1). To minimize water usage during product purification, the work-up procedure focused on centrifugation over classic dialysis. Through reaction optimization, we found that while 5 min of ball-milling was insufficient to thoroughly mix the substrates and produce a uniform reaction mixture for characterization, 10 and 30 min milling both led to the formation of aminoalkylated materials with high DS after a brief aging period of 3 h.

The DS, calculated based on the number of anhydroglucose unit of the reaction substrate (Fig. S1), was calculated at 0.80 (3.31 mmol g^{-1} amine content), when the S_N2-type

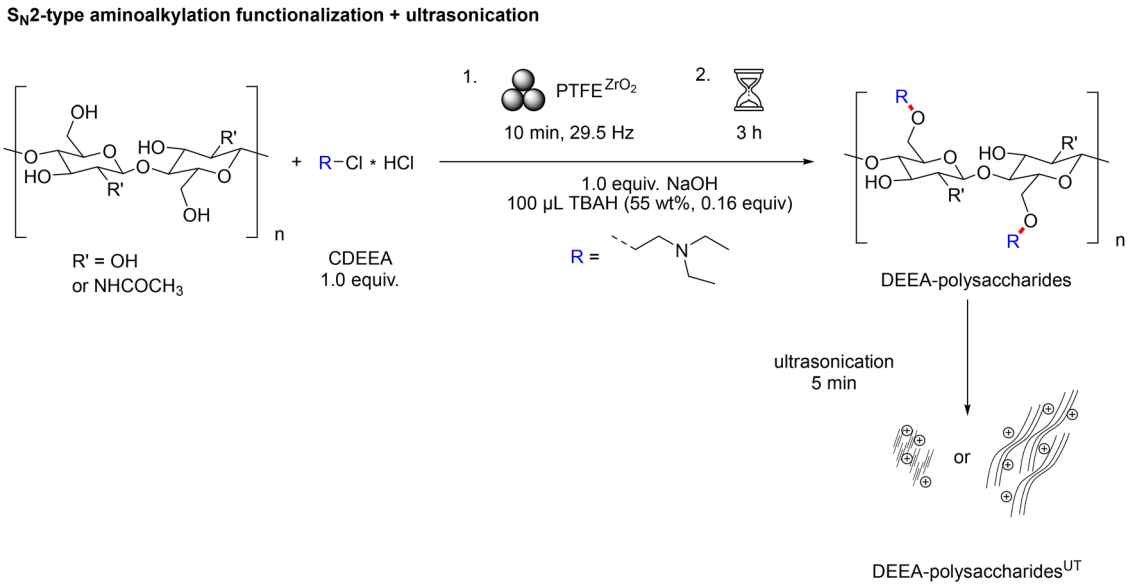

Scheme 1 Mechanochemical and aging based synthesis of DEEA-MCC, DEEA-SBKP, and DEEA-chitin through S$_N$2-type aminoalkylation of polysaccharide substrate with *in situ*-generated CDEEA electrophile, followed by ultrasonication defibrillation to produce cationic nanopolysaccharides. Typical experimental conditions: cellulose or chitin (1.3 mmol), 2-chloro-*N*,*N*-diethylethylamine hydrochloride (1.3 mmol), sodium hydroxide (1.3 mmol) were loaded into a PTFE jar with a 7 mm ZrO_2 ball and milled for 10 min at 29.5 Hz under LAG condition with 100 µL TBAH solution (53.5–56.5 wt%). The PTFE jar containing the reaction mixture was kept sealed and aged for 3 h at room temperature. For defibrillation, the purified dispersion after 4 rounds of centrifugation in DI water was diluted to 0.5 wt% followed by ultrasonication.

aminoalkylation was performed on MCC using the condition developed in our previous study with chitosan and CDMEA, *i.e.* MCC milled with CDEEA for 30 min followed by 2 d of RT aging.[81] When CDEEA was used as the electrophile instead of CDMEA, the DS of MCC was significantly improved, suggesting the possibility of even milder reaction conditions. This could be done by either minimizing the milling time to reduce amorphization of the polysaccharide substrate during mechanochemical functionalization, or by shortening the aging time to enable faster synthesis of the desired products. This second round of optimization yielded positive results: 30 min of milling and 3 h of aging afforded a product with a DS of 0.75 or an amine content of 3.16 mmol g^{-1}. Attempts on further shortened milling time of 10 min still managed to yield material with a DS of 0.84 (3.41 mmol g^{-1} amine content) with 48 h of aging, or a DS of 0.73 (3.11 mmol g^{-1} amine content) after 3 h of aging, all higher than any DS reported in the past (2.31 mmol g^{-1}).[35] The reoptimization on the S$_N$2-type aminoalkylation with CDEEA delivered two major benefits to the synthesis of amine-functionalized polysaccharide in: (1) reducing the crystallinity loss due to extended ball-milling (see SI S2.e),[76] and (2) reducing the total time required to synthesize the material from days to several hours that is usually required in the conventional dispersion-based methods.

Based on our past work[81] and considerations on the S$_N$2 mechanism of this reaction, we propose a mechanism shown in Scheme 2. CDEEA·HCl is first deprotonated by the stoichiometric amount of NaOH, forming an electrophile. The primary

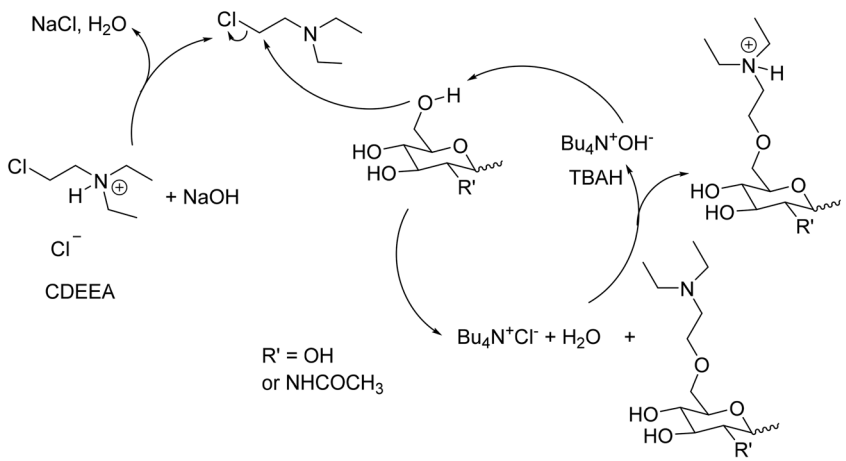

Scheme 2 Reaction mechanism proposal for the mechanochemical and aging based synthesis of DEEA-MCC, DEEA-SBKP, and DEEA-chitin.

alcohol of the polysaccharide is activated by the catalytic amount of TBAH, and reacts with the electrophile, realizing the etherification of the polysaccharide. TBAH is then regenerated through the protonation of the aminated polysaccharide.

Following reaction optimization on MCC, we turned to PG chitin and wood pulp as starting materials to produce cationic nanomaterials. Specifically, 10 min milling (29.5 Hz) of PG chitin along CDEEA·HCl and NaOH under LAG condition with TBAH solution, followed by 3 h of RT aging gave DEEA-chitin with DS of 0.79 (2.79 mmol g^{-1} ammine content, Fig. S3). For wood pulp, we selected once-dried soft bleached kraft pulp (SBKP) as our substrate. Conventional dispersion-based syntheses typically use never-dried pulp,[82] but mechanochemical synthesis requires access to high surface-to-volume ratio, solid-state starting materials. Further treatment, namely dispersion and freeze-drying turned the dense, once-dried SBKP into a fluffy material conducive to efficient ball-milling (see Fig. S5). We then milled this pretreated SBKP with CDEEA·HCl and NaOH under LAG condition with TBAH solution at 29.5 Hz for 10 min, followed by 3 h RT aging in the grinding jars. The reaction mixture obtained from the synthesis prior to purification was a uniform powder mixture with no distinct SBKP fiber left. Furthermore, the successful synthesis of DEEA-SBKP with DS of 0.70 (3.02 mmol g^{-1} amine content) was confirmed by ssNMR spectroscopy (Fig. S2). It is worth noting that we have not been able to perform direct degree of polymerization (DP) measurement on our products, as the introduction of high amine content onto the polysaccharide substrates significantly alters the polysaccharide's behavior under gel permeation chromatography, preventing a reliable measurement in absence of standards. We can however infer that depolymerization is probably minimal since comparable and unreactive milling conditions resulted in minimal chain scission on chitosan,[79] suggesting that the combined process of mild ball-milling and the non-hydrolyzing S_N2-type reaction is unlikely to cause extensive molecular weight reduction in the substrates.

DEEA-cellulose and chitin defibrillation

The DEEA-functionalized polysaccharides contain 2-(diethylamino)ethoxy groups with an estimated pK_a of 7.5.[83] The high DS obtained in our synthesis suggests high levels of protonation when dispersed in neutral water. This was hypothesized to be the key feature that could facilitate strong electric double layer repulsion, and thus low-energy defibrillation by ultrasonication. The high amine content of the mechanochemically produced material therefore makes them good candidates for cationic nanopolysaccharide synthesis. We used a modified method of defibrillation previously reported for TEMPO-oxidized pulp to defibrillate DEEA-cellulose and chitin.[1,49] It was found that the original morphology of the polymer substrate had a profound impact on the resulting products. A 0.5 wt% water dispersion of DEEA-MCC was sonicated with an ultrasonic homogenizer equipped with a probe with a tip diameter of 12.7 mm (1/2″) and a power output of 111.6 W. The DEEA-MCC dispersion became a non-viscous transparent fluid after 5 min, while the 0.5 wt% water dispersion of DEEA-SBKP gained significant viscosity following 5 min of ultrasonication treatment. These samples were coined DEEA-substrate^{UT}. The transparency of the ultrasonicated material was reported by others as a sign of compete defibrillation.[1] Meanwhile, DEEA-chitin did not disintegrate as easily as DEEA-MCC and DEEA-SBK. The water dispersion remained opaque after 5 min of ultrasonication, suggesting insufficient defibrillation of the starting material. Extending the duration of sonication only had a marginal effect on improving the extent of DEEA-chitin defibrillation. We attribute this lower defibrillation efficiency and poorer water-dispersibility of tertiary amine-modified chitin compared to cellulose. Despite their similar DS, the hydrophobic character, strong interstrand hydrogen bonding and potentially higher crystallinity of DEEA-chitin arising from the retention of C2 acetamide groups under this non-deacetylative modification. All sample dispersions after defibrillation by ultrasonication were centrifuged to remove metal contaminants from ultrasonication, and any remaining, sedimented un-defibrillated material. Fully transparent viscous supernatants of ultrasonication-treated DEEA-MCC (DEEA-MCC^{UT}), DEEA-SBKP (DEEA-SBKP^{UT}), and DEEA-chitin (DEEA-chitin^{UT}) dispersion were diluted to 0.1 wt% in water and analyzed by dynamic light scattering (DLS) and ζ-potential measurement. The dispersion was further diluted to 2×10^{-4} wt% water dispersions for microscopic characterization by transmission electron microscopy (TEM) and atomic force microscopy (AFM).

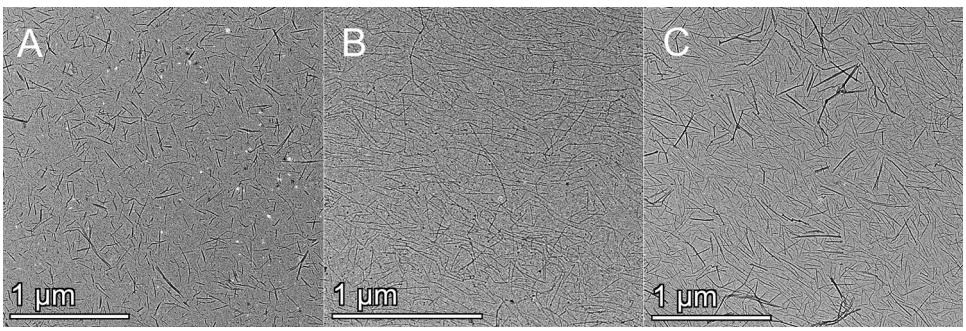

Fig. 1 TEM images of defibrillated samples (A) DEEA-MCC^{UT}, (B) DEEA-SBKP^{UT}, (C) DEEA-chitin^{UT}.

Microscopic characterization of synthesized DEEA-cellulose and chitin nanomaterials

The morphology of the defibrillated nanomaterials was characterized by TEM (Fig. 1). The TEM images of DEEA-MCC^{UT} showed rod-like nanowhiskers with an average length of 225.9 ± 34.2 nm. An average width of 2.3 ± 0.6 nm was measured by AFM, using particle height (Fig. S6 and Table S1). In contrast, DEEA-SBKP^{UT} were densely distributed long fibrils occupying the entire field in the TEM image. To limit the overlap between fibrils and observe the nanomaterials individually, the DEEA-SBKP^{UT} water dispersion was two-fold diluted to 1×10^{-4} wt% for TEM observation, where we confirmed the DEEA-SKBP^{UT} fibrils were *de facto* individually dispersed, with an average length of 1196.4 ± 120.0 nm. The fibril width was measured by AFM to be 2.0 ± 0.5 nm. The length of nanocellulose produced *via* our mechanochemical and aging method were 5 times longer for DEEA-SBKP^{UT}, compared to DEEA-MCC^{UT}, which correlates with what is known of the typical DP of the starting materials. Existing studies show that the DP of MCC is typically below 300 due to acid hydrolysis during production.[84,85] In contrast, the DP of wood pulp ranges from hundreds to 1700, about an order of magnitude larger.[4] On the other hand, the AFM-measured widths were nearly identical, suggesting similar level of defibrillation was achieved with the same amount of ultrasonication, despite differences in the starting materials. The difference between particle length between DEEA-MCC^{UT} and DEEA-SBKP^{UT} was also reflected by the viscosity of respected dispersion at 0.5 wt% with DEEA-SBKP^{UT} becoming a viscous hydrogel, whereas the DEEA-MCC^{UT} dispersion did not appear to become viscous after ultrasonication.

Interestingly, DEEA-chitin^{UT} also had a rod-like whisker morphology, like that of DEEA-MCC^{UT}. Its length, 425.1 ± 52.6 nm measured by TEM, is about double the one of DEEA-MCC^{UT}, while its width, measured by AFM, is comparable at 2.3 ± 0.4 nm. DEEA-chitin^{UT} prepared *via* this approach were longer than typical ChNCs, which are classically in the range of 100–300 nm. The larger particle size of DEEA-chitin^{UT} was also reflected by the high viscosity of its water dispersion. DEEA-chitin^{UT} dispersion contained the most amount of undefibrillated sediments that did not disintegrate with additional ultrasonication. The complex and tightly hydrogen-bonded two- and three-dimensional structures of chitin likely requires higher intensity and energy in the defibrillation process than what ultrasonication can deliver, yet this method uniquely affords access to pure nanomaterials with low energy.[86,87]

With a good understanding of the nanopolysaccharides morphology from microscopy, we turned to the analysis of crystallinity as an important parameter to monitor during the synthesis of nanopolysaccharides because of its role in enabling individualization of the fibers.[88] Additionally, as ball-milling is known to induce loss of crystallinity in polysaccharide materials,[76] we were keen to understand its potential impact on produced nanomaterials.

Whereas powder X-ray diffraction (pXRD) is the most common approach for assessing material crystallinity *via* peak deconvolution, the method is limited by X-ray penetration depths (ranging from a few to a hundred microns) as well as the semicrystalline nature of polysaccharides, which introduces sampling bias and deconvolution errors.[89–93] ^{13}C magic angle spinning ssNMR spectroscopy was thus first selected as a well-established analytical method for cellulose crystallinity characterization. In this method, crystalline (δ 86–90 ppm) and amorphous C4 (δ 83–85 ppm) in cellulose can be resolved for cellulose I and cellulose II polymorphs.[93–96] This method however does not apply to α-chitin as effectively as to cellulose materials, so we will discuss pXRD for all samples subsequently. We acquired the ^{13}C ssNMR spectra of freeze-dried DEEA-MCC^{UT} and DEEA-SBKP^{UT} with the same pulse sequence as performed on DEEA-polysaccharides for DS calculation.

SsNMR spectra are presented in Fig. 2 and CrI calculated from them are noted CrI$_{NMR}$. Starting materials MCC and SBKP

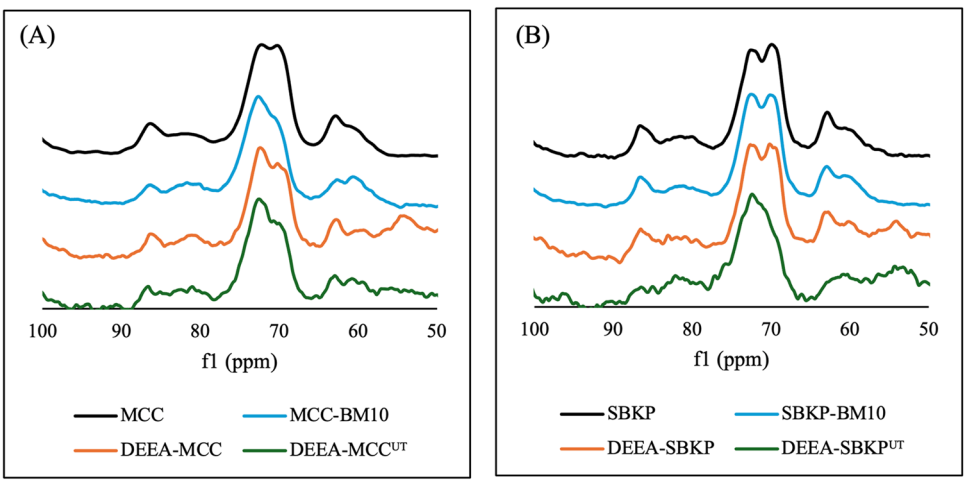

Fig. 2 SsNMR spectra of cellulose samples: starting materials, material milled neat for 10 min (BM10), aminoalkylated DEEA-substrates, and defibrillated DEEA-substrate^{UT} (A) MCC, (B) SBKP.

featured a CrI_{NMR} of 52.1% and 47.4% respectively (Fig. 2), aligning with previously reported value for soft wood pulp around 45%.[94] CrI_{NMR} of DEEA-MCC and DEEA-SBKP were 53.3% and 46.5% respectively, with virtually no difference to the unmodified substrate. This reveals that during the synthesis of the DEEA-nanopolysaccharides, the overall crystallinity of pristine polysaccharides was mostly preserved. This could be attributed to the LAG condition and the reagents added to the jars acting as lubricant during ball-milling, reducing the extent of mechanical amorphization that would have been induced in comparison to the neat milling controls. In contrast, when MCC underwent 10 min of neat milling in the PTFE jar, its CrI_{NMR} dropped to a low 35.0%. After ultrasonication, the crystallinity dropped a little, reaching 51.7% and 39.8% for DEEA-MCC^{UT} and DEEA-SBKP^{UT} respectively. This decrease was attributed to the removal of bundled crystalline surfaces during defibrillation, as previously reported by Daicho *et al.*[93]

We performed the same analysis with pXRD and provide a full discussion of CrI_{XRD} in Discussion S2 and Fig. S4. All CrI_{XRD} values are higher than CrI_{NMR}, and show similar trends. Reference MCC and SBKP had CrI_{XRD} values of 65.4% and 67.8%, respectively dropping to 53.0% and 60.3%, after 10 min neat milling. DEEA-modification before ultrasonication reduced CrI_{XRD} of MCC by only 7.2 pt% to 58.2%, but DEEA-SBKP fell more sharply to 41.0%. As discussed above, NMR spectroscopy remains a more reliable method for this analysis. For chitin, the only available crystallinity analysis method is pXRD (Fig. 3). During defibrillation, DEEA-MCC saw the largest CrI_{XRD} drop (−10 pt% to 45.6%), while DEEA-SBKP hardly changed (43.2%). Evolution of the XRD patterns suggests a partial transformation of cellulose I into cellulose II,[97] possibly the consequence of amine-assisted dissolution/reorganization.[55,94]

Starting material PG chitin had a relatively higher CrI_{XRD} value of 82.8%. Surprisingly and contrary to cellulose, 10 min neat milling saw a small drop to 73.6%, while DEEA-modification before ultrasonication sharply reduced CrI_{XRD} to 57.7% (Fig. 3). For DEEA-chitin^{UT}, CrI_{XRD} decreased modestly (57.7% → 53.7%) but diffraction patterns also shifted, attributed to bulky DEEA groups causing partial crystal reorganization akin to the one seen during chitin deacetylation.[98–101] The CrI_{XRD} of DEEA-chitin^{UT} was lower than the one of reported ChNCs produced *via* ammonium persulfate (APS) oxidation in solution at 75.9%[101] or by a high-humidity shaker aging (HHSA) method at 68%.[72] It is important to note though that DEEA-chitin^{UT} are significantly thinner (2.3 ± 0.4 nm, AFM) than past reports of solution-based APS-oxidized ChNCs (4.6 ± 0.1 nm) or solid-state-based one (8 ± 3 nm).

It is important to note that both pXRD and ssNMR spectroscopy are solid-state characterization techniques that assess materials in their dried form. There may be structural ordering here that differs from arrangement found in DEEA-nanopolysaccharides as they exist in water dispersion. As S_N2-type aminoalkylation functionalized native polysaccharide substrates, it also disrupted interfacial hydrogen bonding within the bulk material, altering the extent of structural ordering and potential recrystallization upon drying. This behavior differs from other existing nanopolysaccharide systems such as carboxylated or acid-hydrolyzed variants.[22,24] Accordingly, the crystallinity data presented in this study should be interpreted primarily as a tool for tracking relative changes in the CrI of DEEA-nanopolysaccharides throughout the production process, rather than as a basis for direct comparison with other material types.

DLS and ζ-potential characterization of synthesized DEEA-cellulose and chitin nanomaterials

The cationization through DEEA-functionalization was confirmed by DLS and ζ-potential measurements (see Table 1). Since DEEA-functionalization introduced 2-(diethylamino)ethoxy groups along the polysaccharide backbone, poly(2-(diethylamino)ethyl

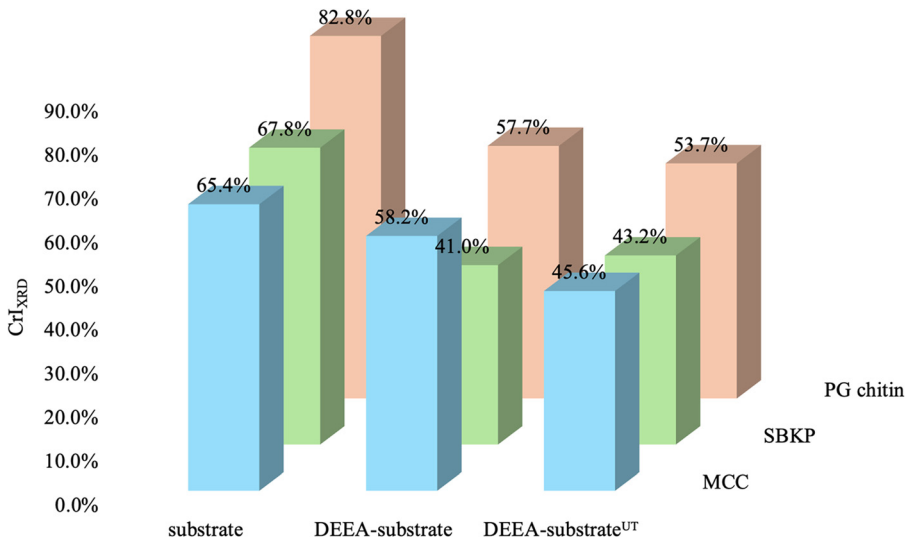

Fig. 3 CrI_{XRD} in polysaccharides (MCC, SBKP and PG chitin) prior reaction (substrate), after mechanochemical/aging-based DEEA functionalization and after ultrasonication treatment.

methacrylate), with a pK_a of 7.5, was used as a reference compound to estimate the pK_a of the resulting nanomaterials.[83] The 0.5 wt% water dispersion of DEEA-SBKP elevated the pH of DI water from 5.5 to 6.0, corresponding to over 95% protonation of the grafted amine groups on the surface. The pH value was later increased to 6.2 after being defibrillated to afford the water dispersion of DEEA-SBKP^{UT}.

The water dispersion of defibrillated DEEA-nanopolysaccharides were diluted to 0.1 wt% for DLS characterization. The ζ-potential measured with the DEEA-MCC^{UT} was 58.64 $\pm$ 1.27 mV, providing the sample with great electric double layer repulsion between the CNFs. Upon ultrasonication, this interfacial repulsive force between strands of elementary fibrils afforded colloidal stability for the DEEA-MCC^{UT} dispersions. DEEA-MCC^{UT} had the smallest apparent particle size of 226.3 $\pm$ 2.6 nm among the three nanopolysaccharides, as per DLS measurements, in agreement with the crystallite size measured with TEM. DEEA-SBKP^{UT} and DEEA-chitin^{UT} had very similar ζ-potential of 68.10 and 68.28 mV respectively, higher than that measured for DEEA-MCC^{UT}. The highest ζ-potential for CCNFs at 56.4 mV was reported in 2021 by Tran-Ly *et al.*[40] This new record high ζ-potential measured across DEEA-MCC^{UT}, DEEA-SBKP^{UT}, and DEEA-chitin^{UT} aligned with the high DS achieved by mechanochemical nucleophilic substitution modification. Like DEEA-MCC^{UT}, the apparent particle sizes of DEEA-SBKP^{UT} (1112.6 $\pm$ 27.3 nm) and DEEA-chitin^{UT} (560.3 $\pm$ 38.5 nm) measured by DLS are also consistent with dimensions obtained by TEM.

Unlike the well-established method used in making individualized TEMPO-oxidized CNFs, in this method, there was no need to pretreat the DEEA-SBKP with a high shear homogenizer to reduce the cellulose fibril's particle size prior to defibrillation by ultrasonication.[102] The optical microscopic images of DEEA-SBKP featured swollen sections on the aminoalkylated pulp fibers (Fig. S7) with partial defibrillation prior to complete defibrillation by ultrasonication. This observation can be explained as a ballooning effect caused by chemical modification and mechanical beating during ball-milling,[103–105] and facilitating further defibrillation during ultrasonication. We demonstrate that mechanochemistry allows for the functionalization at the molecular level of complex matrices, such as wood pulp, as seen in the strong correlation between the measured DS and successful defibrillation. The yield of defibrillated nanopolysaccharides was calculated to be 60.7%, 63.7%, and 47.7% for DEEA-MCC^{UT}, DEEA-SBKP^{UT}, and DEEA-chitin^{UT}, respectively. These results align with the observation that DEEA-chitin yielded the highest amount of undisintegrated sediment after ultrasonication.

Table 1 DLS and ζ-potential measurements of DEEA-MCC^{UT}, UT-DEEA-SBKP^{UT}, and DEEA-chitin^{UT} in DI water (pH $\sim$ 6.5)

Sample	Apparent particle size (nm)	Polydispersity index (PDI)	ζ-potential (mV)
DEEA-MCC^{UT}	226.3 $\pm$ 2.6	0.109 $\pm$ 0.028	58.64 $\pm$ 1.27
DEEA-SBKP^{UT}	1112.6 $\pm$ 27.3	0.263 $\pm$ 0.012	68.10 $\pm$ 1.43
DEEA-chitin^{UT}	560.3 $\pm$ 38.5	0.276 $\pm$ 0.016	68.28 $\pm$ 5.09

pH-Responsiveness and potential applications

Unlike quaternary ammonium-modified CCNFs,[35–43] which are non-pH-responsive and remain water-dispersible across the entire pH range, the tertiary amine-modified CCNFs produced in present study exhibited pH-dependent behavior. The DEEA-SBKP^{UT} water dispersion at 0.5 wt% was taken for the pH-responsiveness test. The pH value of the transparent dispersion was adjusted by gradual addition of 1.0 M NaOH solution with vigorous stirring with a magnetic stirrer. By bringing up the pH value to 8.5 from the initial 6.2, stirring slowed and stopped as dispersion came a rigid gel. This gelation behavior was consistent with the assumption of the pK_a value of the 2-(diethylamino)ethoxy groups grafted onto the substrate of DEEA-SBKP^{UT}. Based on the estimated pK_a of 7.5, the recorded pH change corresponded to a steep decline of protonation degree at the surface of the fibrils from over 90% to 9%, causing a drop in colloidal stability. Therefore, the dispersion collapsed into a hydrogel with long DEEA-SBKP^{UT} fibers heavily entangled with others. Slowly adding 1.0 M HCl solution loosened the DEEA-SBKP^{UT} hydrogel, allowing magnetic stirring to resume, which gradually returned the water dispersion to slightly acidic pH 6.0. However, the obtained water dispersion after acidification was noticeably opaque and contained residual hydrogel fragments in comparison to the freshly defibrillated DEEA-SBKP^{UT} water dispersion, likely due to the agglomeration of the CNFs. Although not fully reversible, the DEEA-SBKP^{UT} prepared in this study by mechanochemistry and aging demonstrated pH-responsive governed by the grafted functional groups. Given the close proximity of the pK_a values of DMEA (7.4) and DEEA (7.5) when grafted onto polysaccharides,[83] the pH-regulated dispersibility and partially reversible gelation of DEEA-nanopolysaccharides could also be triggered by CO_2.[81,106] Unlike mineral acids or bases, CO_2 does not cause salt accumulation between cycles.[107] The pH-responsiveness of DEEA-nanopolysaccharides in water dispersions offers unique opportunities that are not accessible with quaternized cationic nanopolysaccharides, which remain permanently charged and therefore lack reversible dispersibility control. This tunable behavior enables potential applications as surfactants,[108] adsorbents,[109] or emulsifiers.[17,110,111] The high amine loading and pH-responsiveness of the synthesized DEEA-nanopolysaccharides can also impart matrix affinity in the design of on-demand biobased materials such as membranes,[37,112] or in composite materials either as supports,[113] or fillers.[114] In the meantime, the variety of polysaccharide substrates available for this synthesis enables application-oriented material design. For example, the shorter, more rigid, and more hydrophobic ChNCs may provide higher emulsification capacity,[115] whereas the longer, more flexible, and more hydrophilic CNFs are better suited as rheology modifiers.[116] Beyond DEEA-nanopolysaccharides, the surface properties of the nanopolysaccharides obtained by this method

are tunable through the use of different chloroalkyl electrophiles, enabling unlimited customizable design.

Conclusion

In this article, we showcase a pathway to produce pH responsive cationic polysaccharides with high DS through mechanochemistry and aging while preserving high crystallinity, directly from native polysaccharide and without the need for energy intense defibrillation. With the developed method, we successfully synthesized tertiary aminated cellulose pulp (DEEA-SBKP) achieving a DS of 0.70 (amine content 3.02 mmol g^{-1}). This rapid and clean process afforded individualized CCNFs after simple ultrasonication, requiring less than 4 h from starting material to purified nanopolysaccharides. We characterized the CCNFs by microscopy and DLS, revealing a high aspect ratio fibril morphology with average length around 1.2 μm and width of 2.0 nm. A measured ζ-potential of 68.10 ± 1.43 mV promoted defibrillation during ultrasonication of DEEA-SBKP particles. With MCC and PG chitin, two starting substrates in powder form, the method afforded cationic CNCs and ChNCs with high ζ-potential like synthesized CCNFs. The entire procedure produced crystalline nanopolysaccharides with process mass intensity (PMI) around 4.0 if not counting purification (~27 000 with dialysis, ~1000 with centrifugation). This class of new cationic nanopolysaccharides opens new investigation in their physicochemical properties including mechanical, optical, adsorption, and self-assembly properties, potentially providing a new route for polysaccharide biomass valorization.

Experimental

Materials

Cellulose (microcrystalline, average particle size 50 μm) was purchased from Thermo Fisher Scientific (Fair Lawn, NJ, USA). Chitin (from shrimp shell, practical grade), 2-chloro-*N*,*N*-dimethylethylamine hydrochloride (99%), 2-chloro-*N*,*N*-diethylethylamine hydrochloride (99%), 3-dimethylamino-1-propyl chloride hydrochloride (96%), tetrabutylammonium hydroxide solution (53.5–56.5 wt% in H_2O), were purchased from Sigma-Aldrich Co. L.L.C. (St. Louis, MO, USA). Sodium hydroxide (for analysis, micropearls) was purchased from Fisher Scientific L.L.C. (Ottawa, ON, Canada). Soft bleached kraft pulp was kindly provided by Nippon Paper Industries (Tokyo, Japan).

Milling

In the following procedures, a Retsch MM 400 mixer mill was used, with polytetrafluoroethylene (PTFE) SmartSnap Jars (15 mL) manufactured by Form-Tech Scientific (Canada), equipped with 7 mm balls made of zirconia.

Material purification

After milling and aging, the reaction mixture was dispersed in 40 mL of DI water and transferred to a Falcon™ 50 mL High Clarity Conical Centrifuge Tubes. The samples were then purified by 4 cycles of centrifugation with a Thermo Scientific™ Sorvall™ Legend™ XF Centrifuge. The resulting purified DEEA-polysaccharides in the sediment were then freeze-dried for characterization.

DEEA-polysaccharide defibrillation

Instead of drying, purified DEEA-polysaccharides were diluted to 0.5 wt% water dispersion, and sonicated with an ultrasonic homogenizer manufactured by Branson Ultrasonics (Shanghai) Co., Ltd and a probe with a tip diameter of 12.7 mm (1/2″) at a power output of 111.6 W. All sample dispersions after defibrillation by ultrasonication were centrifuged at 8000 rpm to remove metal contaminants from ultrasonication, as well as the remaining un-defibrillated material that sedimented together.

Analysis – characterization – equipment details and methods.

^{13}C magic angle spinning nuclear magnetic resonance (MAS-NMR) spectroscopy. Experimental samples were freeze-dried on a lab lyophilizer before characterization. NMR spectra were recorded on a Varian VNMRS operating at 400 MHz for the solid-state ^{13}C acquisition using a 4 mm double-resonance Varian Chemagnetics T3 probe. A contact time of 1000 μs and a recycle delay of 3 s were used to acquire quantitative spectra. Five hundred scans were acquired of each sample for a total time of 1.5 h.

Transmission electron microscopy. Samples were prepared by solution suspension and drop casted onto a plasma cleaned Cu grid with a carbon backing from Electron Microscopy Sciences. Grids were plasma cleaned with a Pelco easiGlow Glow Discharge Cleaning System, using a negative glow discharge at 25 mA over 45 s. Brightfield micrograph images and energy dispersive X-ray scans were taken on a Thermo Scientific Talos F200X S/TEM operated at 200 keV, with high brightness XFEG Schottky source. Energy dispersive spectroscopy (EDS) was performed with a SuperX G2 energy dispersive spectroscopy detector comprising four windowless SSDs, dwell time 20 μs per pixel and probe current 236 pA. Data was collected with and processed using Velox software; fiber dimensions were measured using ImageJ software.

Atomic force microscopy. 10 μL of sample water dispersion at 2×10^{-4} wt% was drop casted onto a freshly cleaved Muscovite Mica (15 × 15 mm^2, V-2 Quality, Electron Microscopy Sciences, PA, USA), dried in a desiccator under vacuum for 48 h prior to characterization. Surface morphology of samples was analyzed using a Cypher VRS scanning probe microscope equipped with an ARC2 controller (Asylum Research – Oxford Instruments, Santa Barbara, USA) in tapping mode in air under ambient conditions using ACTA probes (AppNano, Mountain View, USA) with nominal spring constant, frequency and radius of curvature of 37 N m^{-1}, 300 kHz and 6 nm, respectively. All images were scanned over ranges of 5 × 5 or 10 × 10 μm^2 at a scan rate of 1 Hz. Processing and data analysis was done using MountainsSPIP v10.3.10931 (Digital Surf, Besançon, France). Images were levelled a flattening operator with structure

exclusion. A particle analysis study with threshold detection identified and extracted fibers for feature-specific measurements. Contiguous particles were segmented using a split particle function and the average Z value of all points within the particles were measured.

Powder X-ray diffraction. Experimental samples were freeze-dried on a lab lyophilizer before characterization. The loose fibril-like samples were loaded onto a Si low background sample holder with minimal vacuum grease. X-ray diffraction spectra were acquired using a Bruker D8 Advance X-ray diffractometer equipped with a CuKα filament, scanned with a 2θ range between 5–50° with an increment of 0.02°.

Dynamic light scattering (DLS) and phase analysis light scattering (PALS). Dynamic light scattering and the zeta potential (ζ-potential) of the samples (1 mg mL^{-1}) in water were determined using a Zetasizer Nano-ZS (Malvern Instruments, Malvern, UK) in triplicate. The DLS measurement was taken at 90° at 25 °C with continuous size distribution for a duration of 120 s each after an equilibration time of 300 s. The PALS measurement was taken with a BI-SREL – solvent-resistant electrode (1250 μL) at 25 °C for 30 cycles in Smoluchowski model.

PDI is the standard deviation (or half-width max) compared to the mean:

$$\mathrm{PDI} = \left(\frac{\text{std. dev.}}{\text{mean}}\right)^2$$

Thus, for colloidal or nanomaterial suspensions, a 'perfect' monodisperse solution would be close to 0, with 0.1–0.4 PDI being a generally monodisperse suspension with little to no aggregation.

Author contributions

The manuscript was written through the contributions of all authors. All authors have given approval to the final version of the manuscript.

Conflicts of interest

There are no conflicts to declare.

Abbreviations

AFM	Atomic force microscopy
APS	Ammonium persulfate
CCNFs	Cationic cellulose nanofibers
CDEEA	2-Chloro-*N*,*N*-diethylethylamine
CDMEA	2-Chloro-*N*,*N*-dimethylethylamine
CDMPA	3-Chloro-*N*,*N*-dimethylpropylamine
ChNC	Chitin nanocrystal
ChsNCs	Chitosan nanocrystals
CNC	Cellulose nanocrystal
CNFs	Cellulose nanofibers
CrI	Crystallinity index
CrI_{NMR}	^{13}C magic angle spinning nuclear magnetic resonance calculated crystallinity index
CrI_{XRD}	Powder X-ray diffraction calculated crystallinity index
DEEA	Diethylethylamine
DI	Deionized
DLS	Dynamic light scattering
DP	Degree of polymerization
DS	Degree of substitution
GTMAC	Glycidyltrimethylammonium chloride
HHSA	High-humidity shaker aging
HP	High-pressure
LAG	Liquid-assisted grinding
MCC	Microcrystalline cellulose
PALS	Phase Analysis Light Scattering
PDI	Polydispersity index
PFAS	Perfluoroalkyl and polyfluoroalkyl substances
PG	Practical grade
PTFE	Polytetrafluoroethylene
pXRD	Powder X-ray Diffraction
RAM	Resonant acoustic mixing
RT	Room temperature
SBKP	Soft bleached kraft pulp
ssNMR	^{13}C magic angle spinning nuclear magnetic resonance
TBAH	Tetrabutylammonium hydroxide
TEM	Transmission electron microscopy
TEMPO	2,2,6,6-Tetramethylpiperidine-1-oxylradical
UT	Ultrasonication-treated

Data availability

The data supporting this article have been included as part of the supplementary information (SI). Supplementary information: comparative bibliography on cationic cellulose nanofiber synthesis, original spectroscopic and microscopic data and process mass intensity calculation. See DOI: **https://doi.org/10.1039/d5nh00597c**.

Acknowledgements

We thank the Natural Science and Engineering Research Council of Canada (NSERC) – Discovery Grant, the Canada Foundation for Innovation (CFI), the Fonds de Recherche du Québec – Nature et Technologies (FRQNT) – the Centre for Green Chemistry and Catalysis (CGCC), the Mitacs Globalink Research Award (G. Y.), JST CREST (grant number JPMJCR22L3), JST ASPIRE (grant number JPMJAP2310), McGill University, including the Heather Munroe-Blum Fellowships in Green Chemistry and Graduate Mobility Award (G. Y.) and Tokyo University, including the Visiting Professorship program (A. M.) for their financial support. We thank the Facility for Electron Microscopy Research (FEMR) of McGill University for help in data collection and Ms Mohini Ramkaran at the MC^2 facility at McGill University for help in acquiring AFM data.

References

1 T. Saito, Y. Nishiyama, J.-L. Putaux, M. Vignon and A. Isogai, Homogeneous Suspensions of Individualized Microfibrils from TEMPO-Catalyzed Oxidation of Native Cellulose, *Biomacromolecules*, 2006, **7**(6), 1687–1691, DOI: 10.1021/bm060154s.

2 H. P. S. Abdul Khalil, Y. Davoudpour, M. N. Islam, A. Mustapha, K. Sudesh, R. Dungani and M. Jawaid, Production and modification of nanofibrillated cellulose using various mechanical processes: A review, *Carbohydr. Polym.*, 2014, **99**, 649–665, DOI: 10.1016/j.carbpol.2013.08.069.

3 A. C. Corrêa, E. de Morais Teixeira, L. A. Pessan and L. H. C. Mattoso, Cellulose nanofibers from curaua fibers, *Cellulose*, 2010, **17**(6), 1183–1192, DOI: 10.1007/s10570-010-9453-3.

4 D. Klemm, B. Heublein, H.-P. Fink and A. Bohn, Cellulose: Fascinating Biopolymer and Sustainable Raw Material, *Angew. Chem., Int. Ed.*, 2005, **44**(22), 3358–3393, DOI: 10.1002/anie.200460587.

5 H. Liimatainen, M. Visanko, J. Sirviö, O. Hormi and J. Niinimäki, Sulfonated cellulose nanofibrils obtained from wood pulp through regioselective oxidative bisulfite pre-treatment, *Cellulose*, 2013, **20**(2), 741–749, DOI: 10.1007/s10570-013-9865-y.

6 F. Rol, M. N. Belgacem, A. Gandini and J. Bras, Recent advances in surface-modified cellulose nanofibrils, *Prog. Polym. Sci.*, 2019, **88**, 241–264, DOI: 10.1016/j.progpolymsci.2018.09.002.

7 M. Ghanadpour, F. Carosio, P. T. Larsson and L. Wågberg, Phosphorylated Cellulose Nanofibrils: A Renewable Nanomaterial for the Preparation of Intrinsically Flame-Retardant Materials, *Biomacromolecules*, 2015, **16**(10), 3399–3410, DOI: 10.1021/acs.biomac.5b01117.

8 A. Ashori, M. Babaee, M. Jonoobi and Y. Hamzeh, Solvent-free acetylation of cellulose nanofibers for improving compatibility and dispersion, *Carbohydr. Polym.*, 2014, **102**, 369–375, DOI: 10.1016/j.carbpol.2013.11.067.

9 S. Doobary, V. Apostolopoulou-Kalkavoura, A. P. Mathew and B. Olofsson, Nanocellulose: New horizons in organic chemistry and beyond, *Chem*, 2024, **10**(11), 3279–3293, DOI: 10.1016/j.chempr.2024.09.007.

10 A. Šturcová, G. R. Davies and S. J. Eichhorn, Elastic Modulus and Stress-Transfer Properties of Tunicate Cellulose Whiskers, *Biomacromolecules*, 2005, **6**(2), 1055–1061, DOI: 10.1021/bm049291k.

11 R. Mark, *Cell wall mechanics of tracheids*, New Haven Yale University Press, 1967, p. 310.

12 A. Dufresne, *Nanocellulose: from nature to high performance tailored materials*, Walter de Gruyter GmbH & Co KG, 2017.

13 S. Ishioka, N. Isobe, T. Hirano, N. Matoba, S. Fujisawa and T. Saito, Fully Wood-Based Transparent Plates with High Strength, Flame Self-Extinction, and Anisotropic Thermal Conduction, *ACS Sustainable Chem. Eng.*, 2023, **11**(6), 2440–2448, DOI: 10.1021/acssuschemeng.2c06344.

14 Q.-F. Guan, H.-B. Yang, Z.-M. Han, L.-C. Zhou, Y.-B. Zhu, Z.-C. Ling, H.-B. Jiang, P.-F. Wang, T. Ma, H.-A. Wu and S.-H. Yu, Lightweight, tough, and sustainable cellulose nanofiber-derived bulk structural materials with low thermal expansion coefficient, *Sci. Adv.*, 2020, **6**(18), eaaz1114, DOI: 10.1126/sciadv.aaz1114.

15 J. Xu, Y. Zou, H. Chen, Z. Wan, A. Takagi, Z. Wang, J. Yu, L. Liu, Y. Lu, Y. Fan and O. J. Rojas, Magnetoresponsive Cellulose Nanofiber Hydrogels: Dynamic Structuring, Selective Light Transmission, and Information Encoding, *ACS Nano*, 2025, **19**(14), 14063–14072, DOI: 10.1021/acsnano.4c18542.

16 T. Yagita, T. Ito, T. Hirano, T. Toyomasu, S. Hasegawa, T. Saito and S. Fujisawa, Evaluating the Emulsifying Capacity of Cellulose Nanofibers Using Inverse Gas Chromatography, *Langmuir*, 2023, **39**(12), 4362–4369, DOI: 10.1021/acs.langmuir.2c03369.

17 Y. Goi, S. Fujisawa, T. Saito, K. Yamane, K. Kuroda and A. Isogai, Dual functions of tempo-oxidized cellulose nanofibers in oil-in-water emulsions: a pickering emulsifier and a unique dispersion stabilizer, *Langmuir*, 2019, **35**(33), 10920–10926.

18 N. Mohammed, N. Grishkewich and K. C. Tam, Cellulose nanomaterials: promising sustainable nanomaterials for application in water/wastewater treatment processes, *Environ. Sci.: Nano*, 2018, **5**(3), 623–658, DOI: 10.1039/c7en01029j.

19 N. Isobe, X. Chen, U.-J. Kim, S. Kimura, M. Wada, T. Saito and A. Isogai, TEMPO-oxidized cellulose hydrogel as a high-capacity and reusable heavy metal ion adsorbent, *J. Hazard. Mater.*, 2013, **260**, 195–201.

20 T. Li, C. Chen, A. H. Brozena, J. Y. Zhu, L. Xu, C. Driemeier, J. Dai, O. J. Rojas, A. Isogai, L. Wågberg and L. Hu, Developing fibrillated cellulose as a sustainable technological material, *Nature*, 2021, **590**(7844), 47–56, DOI: 10.1038/s41586-020-03167-7.

21 S. J. Eichhorn, A. Etale, J. Wang, L. A. Berglund, Y. Li, Y. Cai, C. Chen, E. D. Cranston, M. A. Johns, Z. Fang, G. Li, L. Hu, M. Khandelwal, K. Y. Lee, K. Oksman, S. Pinitsoontorn, F. Quero, A. Sebastian, M. M. Titirici, Z. Xu, S. Vignolini and B. Frka-Petesic, Current international research into cellulose as a functional nanomaterial for advanced applications, *J. Mater. Sci.*, 2022, **57**(10), 5697–5767, DOI: 10.1007/s10853-022-06903-8.

22 A. Isogai, T. Saito and H. Fukuzumi, TEMPO-oxidized cellulose nanofibers, *Nanoscale*, 2011, **3**(1), 71–85, DOI: 10.1039/C0NR00583E.

23 J. Li, X. Wei, Q. Wang, J. Chen, G. Chang, L. Kong, J. Su and Y. Liu, Homogeneous isolation of nanocellulose from sugarcane bagasse by high pressure homogenization, *Carbohydr. Polym.*, 2012, **90**(4), 1609–1613, DOI: 10.1016/j.carbpol.2012.07.038.

24 M. Jonoobi, R. Oladi, Y. Davoudpour, K. Oksman, A. Dufresne, Y. Hamzeh and R. Davoodi, Different preparation methods and properties of nanostructured cellulose from various natural resources and residues: a review,

Cellulose, 2015, **22**(2), 935–969, DOI: 10.1007/s10570-015-0551-0.

25 Y. Nishiyama, Molecular interactions in nanocellulose assembly, *Philos. Trans. R. Soc., A*, 2018, **376**(2112), 20170047, DOI: 10.1098/rsta.2017.0047.

26 A. Isogai, TEMPO-catalyzed oxidation of polysaccharides, *Polym. J.*, 2022, **54**(4), 387–402, DOI: 10.1038/s41428-021-00580-1.

27 T. Saito, M. Hirota, N. Tamura, S. Kimura, H. Fukuzumi, L. Heux and A. Isogai, Individualization of Nano-Sized Plant Cellulose Fibrils by Direct Surface Carboxylation Using TEMPO Catalyst under Neutral Conditions, *Biomacromolecules*, 2009, **10**(7), 1992–1996, DOI: 10.1021/bm900414t.

28 *Cellulose NanoFIbers Market Size, Share, Industry, Forecast and outloom (2024–2031)*, DataM Intelligence, 2024.

29 Y. Noguchi, I. Homma and Y. Matsubara, Complete nanofibrillation of cellulose prepared by phosphorylation, *Cellulose*, 2017, **24**(3), 1295–1305, DOI: 10.1007/s10570-017-1191-3.

30 I. Matsusue, *Cellulose fine fiber-containing material, method for producing the same, and cellulose fine fiber dispersion*, JP6404415B1, 2017.

31 K. Inoue, *Carboxymethylated cellulose nanofiber*, JP6337225B1, 2018.

32 J. Kubo, *Cellulose xanthate nanofiber*, JP6254335B2, 2016.

33 Y. Igarashi, A. Sato, H. Okumura, F. Nakatsubo and H. Yano, Manufacturing process centered on dry-pulp direct kneading method opens a door for commercialization of cellulose nanofiber reinforced composites, *Chem. Eng. J.*, 2018, **354**, 563–568, DOI: 10.1016/j.cej.2018.08.020.

34 S. Hiasa, *Method for producing sulfonated fine cellulose fiber and method for producing sulfonated pulp fiber*, JP6582111B1, 2018.

35 A. Pei, N. Butchosa, L. A. Berglund and Q. Zhou, Surface quaternized cellulose nanofibrils with high water absorbency and adsorption capacity for anionic dyes, *Soft Matter*, 2013, **9**(6), 2047, DOI: 10.1039/c2sm27344f.

36 D. Li, C.-S. Lee, Y. Zhang, R. Das, F. Akter, A. K. Venkatesan and B. S. Hsiao, Efficient removal of short-chain and long-chain PFAS by cationic nanocellulose, *J. Mater. Chem. A*, 2023, **11**(18), 9868–9883, DOI: 10.1039/d3ta01851b.

37 H. Sehaqui, A. Mautner, U. Perez de Larraya, N. Pfenninger, P. Tingaut and T. Zimmermann, Cationic cellulose nanofibers from waste pulp residues and their nitrate, fluoride, sulphate and phosphate adsorption properties, *Carbohydr. Polym.*, 2016, **135**, 334–340, DOI: 10.1016/j.carbpol.2015.08.091.

38 J. Liu, R. Yang, Y. Wang, F. Hua and S. Tong, Cationic cellulose nanofibers with efficient anionic dye adsorption: adsorption mechanism and application in salt-free dyeing of paper, *Cellulose*, 2022, **29**(3), 2047–2061, DOI: 10.1007/s10570-021-04406-4.

39 X. Guo, R. Yang, Y. Wang, S. Ni, C. Cheng, D. Fu and J. Sheng, Cationic cellulose nanofibers/chitosan auxiliary-dominated win-win strategy for paper yarn with superior color and physical performances, *Carbohydr. Polym.*, 2024, **330**, 121833, DOI: 10.1016/j.carbpol.2024.121833.

40 A. N. Tran-Ly, K. J. De France, P. Rupper, F. W. M. R. Schwarze, C. Reyes, G. Nyström, G. Siqueira and J. Ribera, Melanized-Cationic Cellulose Nanofiber Foams for Bioinspired Removal of Cationic Dyes, *Biomacromolecules*, 2021, **22**(11), 4681–4690, DOI: 10.1021/acs.biomac.1c00942.

41 Z. Lu, X. An, H. Zhang, L. Liu, H. Dai, H. Cao, B. Lu and H. Liu, Cationic cellulose nano-fibers (CCNF) as versatile flocculants of wood pulp for high wet web performance, *Carbohydr. Polym.*, 2020, **229**, 115434, DOI: 10.1016/j.carbpol.2019.115434.

42 C. Hou, Y. Wu, T. Wang, X. Wang and X. Gao, Preparation of Quaternized Bamboo Cellulose and Its Implication in Direct Air Capture of CO2, *Energy Fuels*, 2019, **33**(3), 1745–1752, DOI: 10.1021/acs.energyfuels.8b02821.

43 J. A. Sirviö, Cationization of lignocellulosic fibers with betaine in deep eutectic solvent: Facile route to charge stabilized cellulose and wood nanofibers, *Carbohydr. Polym.*, 2018, **198**, 34–40, DOI: 10.1016/j.carbpol.2018.06.051.

44 Z. Khatri, G. Mayakrishnan, Y. Hirata, K. Wei and I.-S. Kim, Cationic-cellulose nanofibers: Preparation and dyeability with anionic reactive dyes for apparel application, *Carbohydr. Polym.*, 2013, **91**(1), 434–443, DOI: 10.1016/j.carbpol.2012.08.046.

45 C. Ji, S. Wu, F. Tang, Y. Yu, F. Hung and Q. Wei, Cationic cellulose nanofiber solid electrolytes: A pathway to high lithium-ion migration and polysulfide adsorption for lithium-sulfur batteries, *Carbohydr. Polym.*, 2024, **335**, 122075, DOI: 10.1016/j.carbpol.2024.122075.

46 M. Muqeet, H. Malik, R. B. Mahar, F. Ahmed, Z. Khatri and K. Carlson, Cationization of Cellulose Nanofibers for the Removal of Sulfate Ions from Aqueous Solutions, *Ind. Eng. Chem. Res.*, 2017, **56**(47), 14078–14088, DOI: 10.1021/acs.iecr.7b03739.

47 J. D. Goodrich and W. T. Winter, α-Chitin Nanocrystals Prepared from Shrimp Shells and Their Specific Surface Area Measurement, *Biomacromolecules*, 2007, **8**(1), 252–257, DOI: 10.1021/bm0603589.

48 H. Yu, Z. Qin, B. Liang, N. Liu, Z. Zhou and L. Chen, Facile extraction of thermally stable cellulose nanocrystals with a high yield of 93% through hydrochloric acid hydrolysis under hydrothermal conditions, *J. Mater. Chem. A*, 2013, **1**(12), 3938, DOI: 10.1039/c3ta01150j.

49 Y. Fan, T. Saito and A. Isogai, Chitin Nanocrystals Prepared by TEMPO-Mediated Oxidation of α-Chitin, *Biomacromolecules*, 2008, **9**(1), 192–198, DOI: 10.1021/bm700966g.

50 T. Jin, T. Liu, E. Lam and A. Moores, Chitin and chitosan on the nanoscale, *Nanoscale Horiz.*, 2021, **6**(7), 505–542, DOI: 10.1039/d0nh00696c.

51 T. Jin, T. Liu, S. Jiang, D. Kurdyla, B. A. Klein, V. K. Michaelis, E. Lam, J. Li and A. Moores, Chitosan nanocrystals synthesis via aging and application towards alginate hydrogels for sustainable drug release, *Green Chem.*, 2021, **23**(17), 6527–6537, DOI: 10.1039/D1GC01611C.

52 S. P. Akhlaghi, M. Zaman, N. Mohammed, C. Brinatti, R. Batmaz, R. Berry, W. Loh and K. C. Tam, Synthesis of amine functionalized cellulose nanocrystals: optimization

and characterization, *Carbohydr. Res.*, 2015, **409**, 48–55, DOI: 10.1016/j.carres.2015.03.009.

53 L. Yue, A. Maiorana, F. Khelifa, A. Patel, J.-M. Raquez, L. Bonnaud, R. Gross, P. Dubois and I. Manas-Zloczower, Surface-modified cellulose nanocrystals for biobased epoxy nanocomposites, *Polymer*, 2018, **134**, 155–162, DOI: 10.1016/j.polymer.2017.11.051.

54 M. Jelkmann, C. Menzel, R. A. Baus, P. Ausserhofer, D. Baecker, R. Gust and A. Bernkop-Schnürch, Chitosan: The One and Only? Aminated Cellulose as an Innovative Option for Primary Amino Groups Containing Polymers, *Biomacromolecules*, 2018, **19**(10), 4059–4067, DOI: 10.1021/acs.biomac.8b01069.

55 N. C. Ellebracht and C. W. Jones, Amine functionalization of cellulose nanocrystals for acid–base organocatalysis: surface chemistry, cross-linking, and solvent effects, *Cellulose*, 2018, **25**(11), 6495–6512, DOI: 10.1007/s10570-018-2043-5.

56 J.-L. Do and T. Friscic, Mechanochemistry: a force of synthesis, *ACS Cent. Sci.*, 2017, **3**(1), 13–19, DOI: 10.1021/acscentsci.6b00277.

57 T. Friščić, New opportunities for materials synthesis using mechanochemistry, *J. Mater. Chem.*, 2010, **20**(36), 7599–7605, DOI: 10.1039/C0JM00872A.

58 Mechano-chemical reaction. 5.0.0 ed., International Union of Pure and Applied Chemistry (IUPAC): 2025.

59 K. Tanaka and F. Toda, Solvent-Free Organic Synthesis, *Chem. Rev.*, 2000, **100**(3), 1025–1074, DOI: 10.1021/cr940089p.

60 G.-W. Wang, Mechanochemical organic synthesis, *Chem. Soc. Rev.*, 2013, **42**(18), 7668–7700, DOI: 10.1039/C3CS35526H.

61 A. Stolle, T. Szuppa, S. E. S. Leonhardt and B. Ondruschka, Ball milling in organic synthesis: solutions and challenges, *Chem. Soc. Rev.*, 2011, **40**(5), 2317–2329, DOI: 10.1039/C0CS00195C.

62 R. R. A. Bolt, J. A. Leitch, A. C. Jones, W. I. Nicholson and D. L. Browne, Continuous flow mechanochemistry: reactive extrusion as an enabling technology in organic synthesis, *Chem. Soc. Rev.*, 2022, **51**(11), 4243–4260, DOI: 10.1039/D1CS00657F.

63 F. Gomollón-Bel, Ten Chemical Innovations That Will Change Our World: IUPAC identifies emerging technologies in Chemistry with potential to make our planet more sustainable, *Chem. Int.*, 2019, **41**, 12–17.

64 J. D. Thorpe, J. Marlyn, S. G. Koenig and M. J. Damha, Synthesis of short DNA and RNA fragments by resonant acoustic mixing (RAM), *RSC Mechanochem.*, 2024, **1**(3), 244–249, DOI: 10.1039/D4MR00009A.

65 D. Farajat, J.-L. Do, P. Forgione, T. Friščić, L. A. Cuccia and C.-J. Li, Shaking Up the Friedländer Reaction: Rapid, Scalable Mechanochemical Synthesis of Polyaryl-Substituted Quinolines, *Adv. Synth. Catal.*, 2024, **366**(24), 5135–5143, DOI: 10.1002/adsc.202400862.

66 F. Qi, R. S. Stein and T. Friščić, Mimicking mineral neogenesis for the clean synthesis of metal–organic materials from mineral feedstocks: coordination polymers, MOFs and metal oxide separation, *Green Chem.*, 2014, **16**(1), 121–132, DOI: 10.1039/C3GC41370E.

67 M. J. Cliffe, C. Mottillo, R. S. Stein, D.-K. Bučar and T. Friščić, Accelerated aging: a low energy, solvent-free alternative to solvothermal and mechanochemical synthesis of metal–organic materials, *Chem. Sci.*, 2012, **3**(8), 2495–2500, DOI: 10.1039/C2SC20344H.

68 P. Tang, C. Jia, Y. Jiang, W. Gong, X. Cao, J. Yang and W. Yuan, Reactivity Studies of Metal–Organic Frameworks under Vapor-Assisted Aging: Structural Interconversions and Transformations, *Eur. J. Inorg. Chem.*, 2016, 5617–5622, DOI: 10.1002/ejic.201600907.

69 M. Đud, O. V. Magdysyuk, D. Margetić and V. Štrukil, Synthesis of monosubstituted thioureas by vapour digestion and mechanochemical amination of thiocarbamoyl benzotriazoles, *Green Chem.*, 2016, **18**(9), 2666–2674, DOI: 10.1039/c6gc00089d.

70 D. Braga, S. L. Giaffreda, F. Grepioni, M. R. Chierotti, R. Gobetto, G. Palladino and M. Polito, Solvent effect in a ''solvent free'' reaction, *CrystEngComm*, 2007, **9**(10), 879–881, DOI: 10.1039/B711983F.

71 D. Cinčić, I. Brekalo and B. Kaitner, Effect of atmosphere on solid-state amine–aldehyde condensations: gas-phase catalysts for solid-state transformations, *Chem. Commun.*, 2012, **48**(95), 11683–11685, DOI: 10.1039/C2CC36357G.

72 T. Jin, T. Liu, F. Hajiali, M. Santos, Y. Liu, D. Kurdyla, S. Régnier, S. Hrapovic, E. Lam and A. Moores, High-Humidity Shaker Aging to Access Chitin and Cellulose Nanocrystals, *Angew. Chem., Int. Ed.*, 2022, **61**(42), e202207206, DOI: 10.1002/anie.202207206.

73 B. G. Fiss, L. Hatherly, R. S. Stein, T. Friščić and A. Moores, Mechanochemical Phosphorylation of Polymers and Synthesis of Flame-Retardant Cellulose Nanocrystals, *ACS Sustainable Chem. Eng.*, 2019, **7**(8), 7951–7959, DOI: 10.1021/acssuschemeng.9b00764.

74 M. Mavlan, T. Chang, R. Feng, J. R. Wilkinson, R. J. Nicholas, N. B. Idahagbon, J. P. Youngblood and A. Wei, Mechanochemical esterification of cellulose nanofibers lyophilized from eutectic water–tert-butanol mixtures, *Cellulose*, 2023, **30**(14), 8805–8817, DOI: 10.1007/s10570-023-05435-x.

75 D. Langerreiter, N. L. Attallah, I. Schlapp-Hackl, M. A. Kostiainen and S. Kaabel, Mechanochemical modification of cellulose nanocrystals by tosylation and nucleophilic substitution, *Green Chem.*, 2024, **26**(18), 9823–9832, DOI: 10.1039/d4gc03378g.

76 T. Di Nardo and A. Moores, Mechanochemical amorphization of chitin: impact of apparatus material on performance and contamination, *Beilstein J. Org. Chem.*, 2019, **15**, 1217–1225, DOI: 10.3762/bjoc.15.119.

77 R. Avolio, I. Bonadies, D. Capitani, M. E. Errico, G. Gentile and M. Avella, A multitechnique approach to assess the effect of ball milling on cellulose, *Carbohydr. Polym.*, 2012, **87**(1), 265–273, DOI: 10.1016/j.carbpol.2011.07.047.

78 T. Di Nardo, C. Hadad, A. Nguyen Van Nhien and A. Moores, Synthesis of high molecular weight chitosan from chitin by mechanochemistry and aging, *Green Chem.*, 2019, **21**(12), 3276–3285, DOI: 10.1039/C9GC00304E.

79 G. Yang, E. Lam and A. Moores, Controlled Chitosan Molecular Weight Reduction by Mechanochemical and Aging-Based Phosphoric Acid Hydrolysis, *ACS Sustainable Chem. Eng.*, 2023, **11**(20), 7765–7774, DOI: 10.1021/acssuschemeng.3c00367.

80 G. Yang, S. Régnier, N. Huin, T. Liu, E. Lam and A. Moores, Mechanochemical and aging-based reductive amination with chitosan and aldehydes affords high degree of substitution functional biopolymers, *Green Chem.*, 2024, **26**(9), 5386–5396, DOI: 10.1039/D4GC00127C.

81 G. Yang, R. S. Korchinsky, J. Sauvé-St-Pierre, P. G. Jessop, E. Lam and A. Moores, Mechanochemical and Aging-Based SN2 Method to Access CO2-Responsive, High-Amine-Loading Chitosan, *ChemSusChem*, 2025, **18**(19), e202501187, DOI: 10.1002/cssc.202501187.

82 Y. Okita, T. Saito and A. Isogai, TEMPO-mediated oxidation of softwood thermomechanical pulp, *Holzforschung*, 2009, **63**(5), 529–535, DOI: 10.1515/HF.2009.096.

83 P. van de Wetering, E. E. Moret, N. M. E. Schuurmans-Nieuwenbroek, M. J. van Steenbergen and W. E. Hennink, Structure−Activity Relationships of Water-Soluble Cationic Methacrylate/Methacrylamide Polymers for Nonviral Gene Delivery, *Bioconjugate Chem.*, 1999, **10**(4), 589–597, DOI: 10.1021/bc980148w.

84 O. Battista and P. Smith, Microcrystalline cellulose, *Ind. Eng. Chem.*, 1962, **54**(9), 20–29.

85 G. Shlieout, K. Arnold and G. Müller, Powder and mechanical properties of microcrystalline cellulose with different degrees of polymerization, *AAPS PharmSciTech*, 2002, **3**(2), 11, DOI: 10.1208/pt030211.

86 L. Bai, L. Liu, M. Esquivel, B. L. Tardy, S. Huan, X. Niu, S. Liu, G. Yang, Y. Fan and O. J. Rojas, Nanochitin: Chemistry, Structure, Assembly, and Applications, *Chem. Rev.*, 2022, **122**(13), 11604–11674, DOI: 10.1021/acs.chemrev.2c00125.

87 R. A. A. Muzzarelli, *Chitin Nanostructures in Living Organisms*, Springer Netherlands, 2011, pp. 1–34.

88 N. Lin, J. Huang and A. Dufresne, Preparation, properties and applications of polysaccharide nanocrystals in advanced functional nanomaterials: a review, *Nanoscale*, 2012, **4**(11), 3274–3294, DOI: 10.1039/C2NR30260H.

89 C. Michaelsen, On the structure and homogeneity of solid solutions: The limits of conventional X-ray diffraction, *Philos. Mag. A*, 1995, **72**(3), 813–828, DOI: 10.1080/01418619508243802.

90 N. Tarannum, Suhani and D. Kumar, Synthesis, characterization and applications of copolymer of β – cyclodextrin: a review, *J. Polym. Res.*, 2020, **27**(4), 89, DOI: 10.1007/s10965-020-02058-9.

91 A. H. Mazurek and A. Szeleszczuk, Review of Applications of Solid-State Nuclear Magnetic Resonance (ssNMR) for the Analysis of Cyclodextrin-Including Systems, *Int. J. Mol. Sci.*, 2023, **24**(4), 3648.

92 J. Liu, R. E. Saw and Y. H. Kiang, Calculation of Effective Penetration Depth in X-Ray Diffraction for Pharmaceutical Solids, *J. Pharm. Sci.*, 2010, **99**(9), 3807–3814, DOI: 10.1002/jps.22202.

93 K. Daicho, T. Saito, S. Fujisawa and A. Isogai, The Crystallinity of Nanocellulose: Dispersion-Induced Disordering of the Grain Boundary in Biologically Structured Cellulose, *ACS Appl. Nano Mater.*, 2018, **1**(10), 5774–5785, DOI: 10.1021/acsanm.8b01438.

94 K. Daicho, K. Kobayashi, S. Fujisawa and T. Saito, Recovery of the Irreversible Crystallinity of Nanocellulose by Crystallite Fusion: A Strategy for Achieving Efficient Energy Transfers in Sustainable Biopolymer Skeletons, *Angew. Chem., Int. Ed.*, 2021, **60**(46), 24630–24636, DOI: 10.1002/anie.202110032.

95 Y. Doi, K. Daicho, N. Isobe, R. Tanaka, S. Kimura, S. Fujisawa and T. Saito, Monitoring crystallite fusion of nanocellulose during colloid condensation, *Cellulose*, 2023, **30**(13), 8287–8297, DOI: 10.1007/s10570-023-05354-x.

96 E. Dinand, M. Vignon, H. Chanzy and L. Heux, Mercerization of primary wall cellulose and its implication for the conversion of cellulose I → cellulose II, *Cellulose*, 2002, **9**(1), 7–18, DOI: 10.1023/A:1015877021688.

97 A. D. French, Idealized powder diffraction patterns for cellulose polymorphs, *Cellulose*, 2014, **21**(2), 885–896, DOI: 10.1007/s10570-013-0030-4.

98 E. Podgorbunskikh, T. Kuskov, D. Rychkov, O. Lomovskii and A. Bychkov, Mechanical Amorphization of Chitosan with Different Molecular Weights, *Polymers*, 2022, **14**(20), 4438.

99 Y. Zhang, C. Xue, Y. Xue, R. Gao and X. Zhang, Determination of the degree of deacetylation of chitin and chitosan by X-ray powder diffraction, *Carbohydr. Res.*, 2005, **340**(11), 1914–1917, DOI: 10.1016/j.carres.2005.05.005.

100 T. Lertwattanaseri, N. Ichikawa, T. Mizoguchi, Y. Tanaka and S. Chirachanchai, Microwave technique for efficient deacetylation of chitin nanowhiskers to a chitosan nanoscaffold, *Carbohydr. Res.*, 2009, **344**(3), 331–335, DOI: 10.1016/j.carres.2008.10.018.

101 T. Jin, D. Kurdyla, S. Hrapovic, A. C. W. Leung, S. Régnier, Y. Liu, A. Moores and E. Lam, Carboxylated Chitosan Nanocrystals: A Synthetic Route and Application as Superior Support for Gold-Catalyzed Reactions, *Biomacromolecules*, 2020, **21**(6), 2236–2245, DOI: 10.1021/acs.biomac.0c00201.

102 T. Saito, R. Kuramae, J. Wohlert, L. A. Berglund and A. Isogai, An Ultrastrong Nanofibrillar Biomaterial: The Strength of Single Cellulose Nanofibrils Revealed via Sonication-Induced Fragmentation, *Biomacromolecules*, 2013, **14**(1), 248–253, DOI: 10.1021/bm301674e.

103 S. Dasgupta, Mechanism of paper tensile-strength development due to pulp beating, *Tappi J.*, 1994, **77**, 158–166.

104 E. Afra, H. Yousefi, M. M. Hadilam and T. Nishino, Comparative effect of mechanical beating and nanofibrillation of cellulose on paper properties made from bagasse and softwood pulps, *Carbohydr. Polym.*, 2013, **97**(2), 725–730, DOI: 10.1016/j.carbpol.2013.05.032.

105 X. Lin, Y. Li, Z. Fang, G. Li, Y. Liu and X. Qiu, Strong Yet Tough Transparent Paper with Superb Foldability, *Small*, 2024, **20**(33), 2400151, DOI: 10.1002/smll.202400151.

106 J. Glasing, P. G. Jessop, P. Champagne and M. F. Cunningham, Graft-modified cellulose nanocrystals as CO2-switchable Pickering emulsifiers, *Polym. Chem.*, 2018, **9**(28), 3864–3872, DOI: **10.1039/C8PY00417J**.

107 M. F. Cunningham and P. G. Jessop, An introduction to the principles and fundamentals of CO2-switchable polymers and polymer colloids, *Eur. Polym. J.*, 2016, **76**, 208–215, DOI: **10.1016/j.eurpolymj.2016.01.036**.

108 Y. Liu, P. G. Jessop, M. Cunningham, C. A. Eckert and C. L. Liotta, Switchable Surfactants, *Science*, 2006, **313**(5789), 958–960, DOI: **10.1126/science.1128142**.

109 Z. Du, S. Deng, Y. Bei, Q. Huang, B. Wang, J. Huang and G. Yu, Adsorption behavior and mechanism of perfluorinated compounds on various adsorbents—A review, *J. Hazard. Mater.*, 2014, **274**, 443–454, DOI: **10.1016/j.jhazmat.2014.04.038**.

110 L. Cai, Y. Wang, J. Zhang, T. Li, S. Song, L. Yu and S. Xia, pH-responsive Pickering emulsions synergistically stabilized by chitin nanocrystals and shellac nanoparticles for astaxanthin delivery, *Food Res. Int.*, 2025, 117090, DOI: **10.1016/j.foodres.2025.117090**.

111 Y. Kaku, S. Fujisawa, T. Saito and A. Isogai, Synthesis of Chitin Nanofiber-Coated Polymer Microparticles via Pickering Emulsion, *Biomacromolecules*, 2020, **21**(5), 1886–1891, DOI: **10.1021/acs.biomac.9b01757**.

112 M. E. Lamm, K. Li, J. Qian, L. Wang, N. Lavoine, R. Newman, D. J. Gardner, T. Li, L. Hu, A. J. Ragauskas, H. Tekinalp, V. Kunc and S. Ozcan, Recent Advances in Functional Materials through Cellulose Nanofiber Templating, *Adv. Mater.*, 2021, **33**(12), 2005538, DOI: **10.1002/adma.202005538**.

113 C. Li, J. Liu, W. Li, Z. Liu, X. Yang, B. Liang, Z. Huang, X. Qiu, X. Li, K. Huang and X. Zhang, Biobased Intelligent Food-Packaging Materials with Sustained-Release Antibacterial and Real-Time Monitoring Ability, *ACS Appl. Mater. Interfaces*, 2023, **15**(31), 37966–37975, DOI: **10.1021/acsami.3c09709**.

114 Q. Cui, X. Huang, X. Dong, H. Zhao, X. Liu and X. Zhang, Self-Healing Bimodal Sensors Based on Bioderived Polymerizable Deep Eutectic Solvent Ionic Elastomers, *Chem. Mater.*, 2022, **34**(23), 10778–10788, DOI: **10.1021/acs.chemmater.2c03105**.

115 S. Fujisawa, R. Tanaka, Y. Hayashi, Y. Yabuhara, M. Kume and T. Saito, Effect of nanocellulose length on emulsion stabilization and microparticle synthesis, *Polym. J.*, 2023, **55**(3), 223–228, DOI: **10.1038/s41428-022-00748-3**.

116 X. Sun, Q. Wu, S. Lee, Y. Qing and Y. Wu, Cellulose Nanofibers as a Modifier for Rheology, Curing and Mechanical Performance of Oil Well Cement, *Sci. Rep.*, 2016, **6**(1), 31654, DOI: **10.1038/srep31654**.

